molecules

MDPI

Article

Anti-Inflammatory Ergosteroid Derivatives from the Coral-Associated Fungi *Penicillium oxalicum* HL-44

Cheng Pang [1,2,†], Yu-Hong Chen [3,†], Hui-Hui Bian [3], Jie-Ping Zhang [2], Li Su [3], Hua Han [2,*] and Wen Zhang [1,2,*]

[1] School of Pharmaceutical Sciences, Zhejiang Chinese Medical University, Gao-Ke Rd., Hangzhou 311402, China
[2] School of Medicine, Tongji University, 1238 Gonghexin Rd., Shanghai 200070, China
[3] Institute of Translational Medicine, Shanghai University, 99 Shangda Rd., Shanghai 200444, China
* Correspondence: hanhua@tongji.edu.cn (H.H.); wenzhang1968@163.com (W.Z.)
† These authors contributed equally to this work.

Abstract: To obtain the optimal fermentation condition for more abundant secondary metabolites, Potato Dextrose Agar (PDA) medium was chosen for the scale-up fermentation of the fungus *Penicillium oxalicum* HL-44 associated with the soft coral *Sinularia gaweli*. The EtOAc extract of the fungi HL-44 was subjected to repeated column chromatography (CC) on silica gel and Sephadex LH-20 and semipreparative RP-HPLC to afford a new ergostane-type sterol ester (**1**) together with fifteen derivatives (**2**–**16**). Their structures were determined with spectroscopic analyses and comparisons with reported data. The anti-inflammatory activity of the tested isolates was assessed by evaluating the expression of pro-inflammatory factors *Tnfα* and *Ifnb1* in Raw264.7 cells stimulated with LPS or DMXAA. Compounds **2**, **9**, and **14** exhibited significant inhibition of *Ifnb1* expression, while compounds **2**, **4**, and **5** showed strong inhibition of *Tnfα* expression in LPS-stimulated cells. In DMXAA-stimulated cells, compounds **1**, **5**, and **7** effectively suppressed *Ifnb1* expression, whereas compounds **7**, **8**, and **11** demonstrated the most potent inhibition of *Tnfα* expression. These findings suggest that the tested compounds may exert their anti-inflammatory effects by modulating the cGAS-STING pathway. This study provides valuable insight into the chemical diversity of ergosteroid derivatives and their potential as anti-inflammatory agents.

Keywords: *Penicillium oxalicum*; coral-associated fungi; ergosteroid derivatives; anti-inflammatory activity

Citation: Pang, C.; Chen, Y.-H.; Bian, H.-H.; Zhang, J.-P.; Su, L.; Han, H.; Zhang, W. Anti-Inflammatory Ergosteroid Derivatives from the Coral-Associated Fungi *Penicillium oxalicum* HL-44. *Molecules* **2023**, *28*, 7784. https://doi.org/10.3390/molecules28237784

Academic Editors: Ericsson Coy-Barrera and Ricardo Calhelha

Received: 21 August 2023
Revised: 24 October 2023
Accepted: 20 November 2023
Published: 26 November 2023

1. Introduction

Marine organisms are a rich source of steroids with potent anti-inflammatory activity. They perform functions by attenuating the activity of the immune system and suppressing inflammation [1]. The ergosteroids are the vast majority of these steroids and construct the main steroid of fungi [2].

Penicillium oxalicum is a frequently isolated fungus exhibiting a wide spectrum of physiological activities that are of relevance in agriculture, biotechnology, food quality assessments, and medicine [3]. Previous chemical investigations of *P. oxalicum* led to the isolation of alkaloids [4,5], polyketides [6,7], meroterpenoids [8,9], and steroids [10,11], exhibiting bioactivities of brine shrimp lethality and anti-*Rhizoctonia Solani*, anti-neuroinflammatory, antipancreatic tumor, anti-HAB (harmful algal bloom), antiviral, and antibacterial properties. *P. oxalicum* is known for its ability in biotransformation. The fungi were found to be able to act as hyperproducers of chitin deacetylase for converting chitin to chitosan, transforming protopanaxadiol-type saponins to ginsenoside compound K, and promoting the biotransformation of ethinylestradiol 1 [12,13].

Research conducted in our group rests on the chemical and pharmacological investigation of secondary metabolites from marine invertebrates and associated fungi. Recently,

we focused on the molecules having immunomodulatory and neuronal modulatory activities. A drimane meroterpenoid characterized by a thioglycerate moiety [14] and a drimane meroterpenoid with a unique borate ring system [15] were obtained from the fungi *Alternaria* sp. ZH-15 associated with the soft coral *Lobophytum crassum* collected from the Dongsha Atoll in the South China Sea. These compounds displayed potential as novel anti-epileptic agents due to their significant inhibitory activities of spontaneous synchronous Ca^{2+} oscillations (SCO) and 4-aminopyridine-induced epileptic discharges in the low micromolar concentration range. Sixteen 9,10-secosteroids were isolated from the gorgonian *Verrucella umbraculum* collected from the Xisha islands in the South China Sea. These compounds exhibited significant suppressive effects on $CD4^+$ T lymphocyte cell differentiation in an in vitro bioassay, representing the first report of 9,10-secosteroids to exhibit immunomodulation activity [16]. As part of ongoing screening for bioactive metabolites from China marine sources, a fungus strain of *P. oxalicum* HL-44 was isolated from the soft coral *Sinularia gaweli* collected from the Xisha area of the South China Sea. Chemical investigation of this fungi led to the isolation of a new ergostane-type sterol ester (**1**) and fifteen known derivatives (**2**–**16**). Their structures were determined with extensive spectroscopic analyses and comparisons with reported data. We investigated the anti-inflammatory activities of these isolates in vitro by examining their effects on the expression of proinflammatory cytokines *Tnfα* and *Ifnb1* in Raw264.7 cells stimulated with LPS or DMXAA. In the present study, we describe the isolation, structure elucidation, and anti-inflammatory activities of these compounds.

2. Results and Discussion

To obtain the optimal fermentation condition, UPLC-MS was employed for the chemical analysis of fungal metabolites produced with strain HL-44 in five candidates of media, including Czapek Dox Agar (CZA) medium, Glucose Peptone Yeast (GPY) medium, PDA medium, Rose Bengal Medium (RBM), and Rice medium. The Total Ion Chromatography (TIC) of the PDA medium showed more abundant metabolites with ion peaks (m/z) in a mass spectrum ranging from 408 to 688. In particular, the ion peak at m/z 663.534 was fairly interesting. Thus, the PDA medium was chosen for the scale-up fermentation of the fungi HL-44.

The fungal strain was then cultivated on the PDA medium for scale fermentation at 28 °C for 28 days and was then extracted ultrasonically with EtOAc to afford a residue after removal of the solvent under reduced pressure [14,15]. The crude extract was subjected to column chromatography (CC) silica gel, Sephadex LH-20, and reversed phase HPLC to afford compounds **1**–**16** (Figure 1). On the basis of spectroscopic techniques (^{1}H-NMR, ^{13}C-NMR) and comparison with data recorded in the references, compounds **2**–**16** were determined as (22*E*,24*R*)-9*α*,15*α*-dihydroxyergosta-4,6,8(14),22-tetraen-3-one (**2**) [17], ganodermaside D (**3**) [18], (22*E*,24*R*)-ergosta-4,6,8(14),22-tetraen-3-one (**4**) [19], isocyathisterol (**5**) [20], herbarulide (**6**) [21], dankasterones A (**7**) [22], (22*E*,24*R*)-ergosta-7,22-dien-3*β*,5*α*-diol-6-one (**8**) [23], (22*E*,24*R*)-ergosta-7,22-dien-3*β*,5*α*,9*α*-trihydroxy-6-one (**9**) [24], (22*E*,24*R*)-3*β*-hydroxyergosta-5,8,22-trien-7-one (**10**) [25], (22*E*,24*R*)-5*α*,9*α*-epidioxyergosta-6,8(14),22-triene-3*β*-ol (**11**) [26], (22*E*, 24*R*)-7*α*-methoxy-5*α*,6*α*-epoxyergosta-8(14),22-dien-3*β*-ol (**12**) [27], (22*E*,24*R*)-6-acetoxy-ergosta-7,22-dien-3*β*,5*α*,6*β*-triol (**13**) [28], (22*E*,24*R*)-5*α*,8*α*-epidioxyergosta-6,9(11),22-trien-3*β*-ol (**14**) [29], (22*E*,24*R*)-5*α*,8*α*-epidioxyergosta-6,22-dien-3*β*-ol (**15**) [30], and demethylincisterol A3 (**16**) [31].

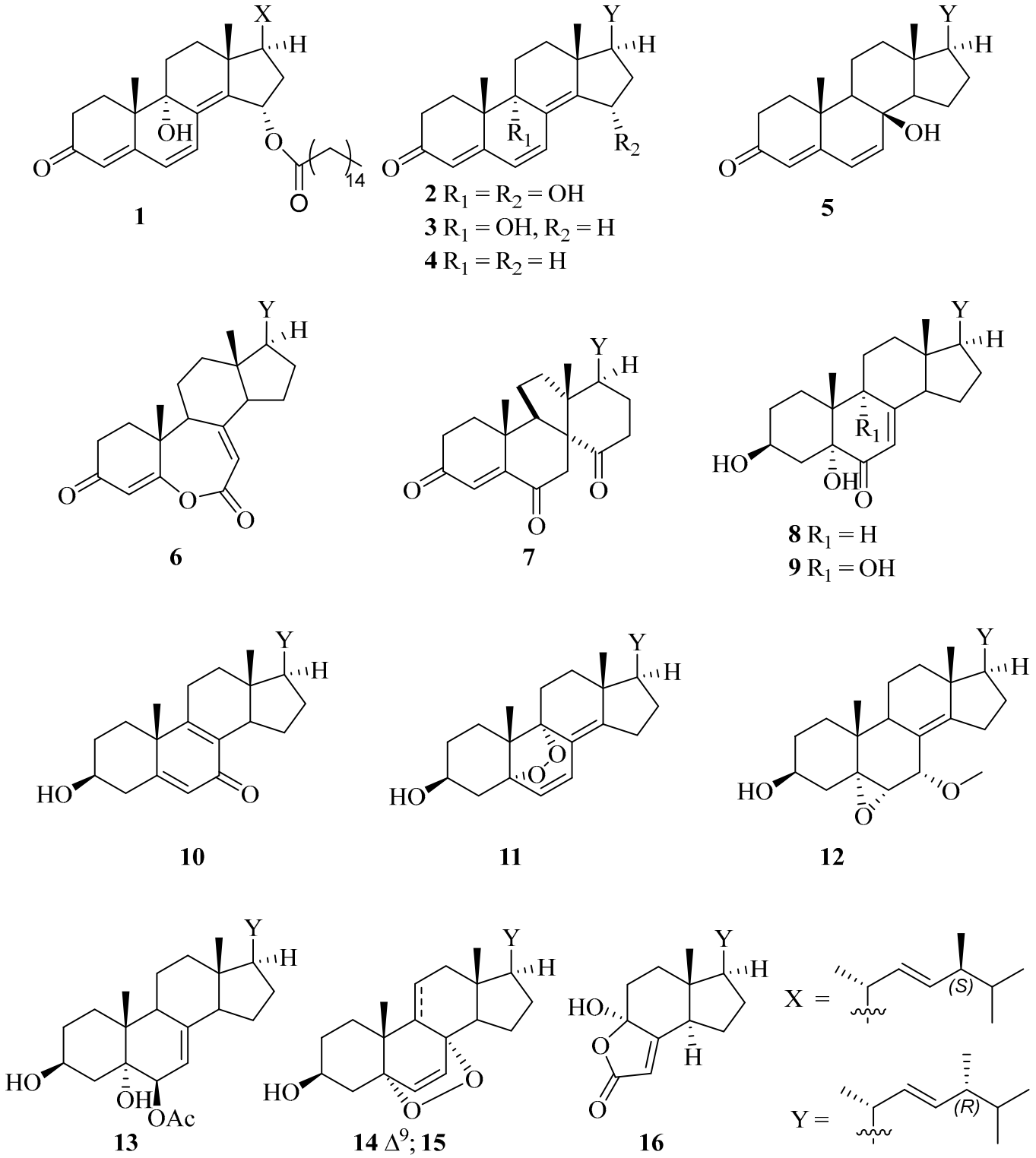

Figure 1. Structures of compounds **1**–**16** isolated from the fungi *P. oxalicum* HL-44**,** having a corresponding *β*-methyl in X or *α*-methyl in Y.

Compound **1** was obtained as an optically yellowish oil. The HRESIMS gave a molecular formula as $C_{44}H_{70}O_4$ on the basis of its pseudomolecular ion peak at *m*/*z* 663.53448 ([M + H]$^+$), indicating 10 degrees of unsaturation. The IR spectrum revealed the presence of a hydroxy group (3344 cm^{-1}) and carbonyl (1733 cm^{-1}) functionalities. The characteristic IR absorptions at 1664 and 1595 cm^{-1} and the strong UV absorptions at 265 and 330 nm

indicated the presence of a large conjugated carbonyl system in this molecule. These observations were in agreement with the NMR data for an oxygenated methine (δ_H 5.81; δ_C 71.8, CH), a tertiary oxygenated carbon atom (δ_C 72.8, C), four pairs of double bonds, one ester carbonyl atom (δ_C 173.6), and one ketone carbonyl atom (δ_C 199.3), taking into account six degrees of unsaturation. The remaining four degrees of unsaturation were due to the ring system in the molecule. Compound **1** resembled **2** in the NMR data (Table 1) except for signals for a palmitoyl moiety, which was supported by the 2D NMR analyses, as shown in Figure 2. The palmitoyl moiety was assigned at C-15 by the distinct HMBC effects of H-15 with C-8, C-13, C-17, and the ester carbonyl atom (C-1′). Compound **1** displayed the same relative configuration as that of **2** in the core structure, as shown in Figure 3. The β-configuration of H-15 was indicated by its NOE correlation with H_3-18. The configuration at C-9 was suggested by comparing its shift value (δ_C 72.8, C) to those reported in the literature (δ_C 72.7/72.8, C) [17,32], indicating that the hydroxy group at C-9 was in the α-configuration. The absolute configuration of C-24 was assigned as *S* in **1** vs *R* in **2** based on the ^{13}C NMR shift values of C-28. The NMR data for C-28 are reported at δ 17.6 $\pm$ 0.1 ppm for 24*R*-isomers and δ 18.0 $\pm$ 0.1 ppm for 24*S*-isomers [16,33]. The presence of a palmitic acid residue was proven with an MS analysis and comparison of the spectroscopic data with those reported data [34]. The existence of the fatty acyl moiety was indicated by the characteristic ^{13}C signals for the ester carbonyl carbon (δ_C 173.6) and ^{1}H signals for triplet methylene at δ_H 2.30, multiplet methylenes at δ_H 1.23–1.30, and a terminal methyl group at δ_H 0.88. The structure of **1** was thus determined as (22*E*,24*S*)-9α,15α-dihydroxyergosta-4,6,8(14),22-tetraen-3-one 15-palmitate, showing a 24*S* configuration vs. 24*R* in **2**. The compound is also characterized by a 15-palmitoyl moiety with respect to a hydroxyl group in **2**.

Table 1. ^{1}H and ^{13}C NMR spectral data of compound **1** in $CDCl_3$. (500 MHz for ^{1}H and 125 MHz for ^{13}C, δ in ppm, *J* in Hz).

Position	δ_C	δ_H (*J* in Hz)	Position	δ_C	δ_H (*J* in Hz)
1	27.5	2.53 m, 1.80 m	19	21.0	1.14 s
2	33.9	2.53 m	20	38.4	2.12 m
3	199.3	-	21	21.3	1.09 d (6.6)
4	127.3	5.91 s	22	134.4	5.19 dd (15.3, 8.2)
5	160.4	-	23	133.5	5.26 dd (15.3, 7.6)
6	126.5	6.13 d (9.8)	24	43.1	1.85 m
7	129.9	6.41 d (9.8)	25	33.1	1.47 m
8	132.0	-	26	20.1	0.83 d (6.7)
9	72.8	-	27	19.7	0.81 d (6.8)
10	42.4	-	28	17.9	0.92 d (6.8)
11	25.6	2.02 m, 1.75 m	1′	173.6	-
12	32.1	2.00 m, 1.72 m	2′	34.7	2.30 t (7.2)
13	44.8	-	3′	25.2	1.61 m
14	154.0	-	4′–13′	29.8–29.3	1.30–1.23 m
15	71.8	5.81 d (7.1)	14′	32.0	1.25 m
16	37.6	1.94 m, 1.72 m	15′	22.8	1.31 m, 1.24 m
17	53.1	1.63 m	16′	14.2	0.88, t (6.6)
18	19.3	0.95 s			

s = singlet; d = doublet; t = triplet; m = multiplet; dd = doublet of doublet.

Derivatives of 15α-hydroxy steroids serve as key intermediates in the production of contraceptives [35,36]. A P450 enzyme, which is composed of the cytochrome P450 hydroxylase and the NADPH-cytochrome P450 reductase (CPR), has been reported to be associated with the 15α-hydroxylation reaction in *P. raistrickii* [37]. *P. raistrickii*-mediated 15α-hydroxylation of D-ethylgonendione is a key step for the production of gestodene [38]. The 9,15-hydroxylated ergosteroid **2** was only reported in *Omphalia lapidescens* [32] and *Ganoderma resinaceum* [17]. The isolation of **1** and **2** suggests that *P. oxalicum* strains have a potential in fungal transformation to afford 15α-hydroxyergosteroid. Compounds **3** and **4**

have a chemical feature of conjugated 4,6,8-trien-3-one and have never been reported in *P. oxalicum*. Compound **6** is a ketodivinyllactone steroid with an unprecedented homo-6-oxaergostane skeleton isolated from the endophytic fungus *Pleospora herbarum* [39] with a structure revision at C24 with a chemical synthesis [21]. Compound **7** was an unprecedented steroid possessing a 13(14→8)*abeo*-8-ergostane skeleton first found in the Halichondria sponge-derived fungus *Gymnacella dankaliensis* [22]. Compound **11**, which features an unusual 1,2-dioxolane moiety, was only reported in *G. capense* [26] and *G. lingzhi* [40]. Although 5*α*,8*α*-epidioxysterols with variations in the side chains were most commonly reported from a number of sources, rare 5*α*,9*α*-epidioxy steroids were mainly isolated from different edible mushrooms [41,42]. The compound showed weak anti-HIV activity and remarkable cytotoxicity against A549 and MCF-7 tumor cell lines. Compound **16** is a highly degraded sterol, and its basic skeleton derives from a dramatic oxidative degradation of the sterol nucleus with the loss of all six carbon atoms of the A ring and the 19-methyl group [43].

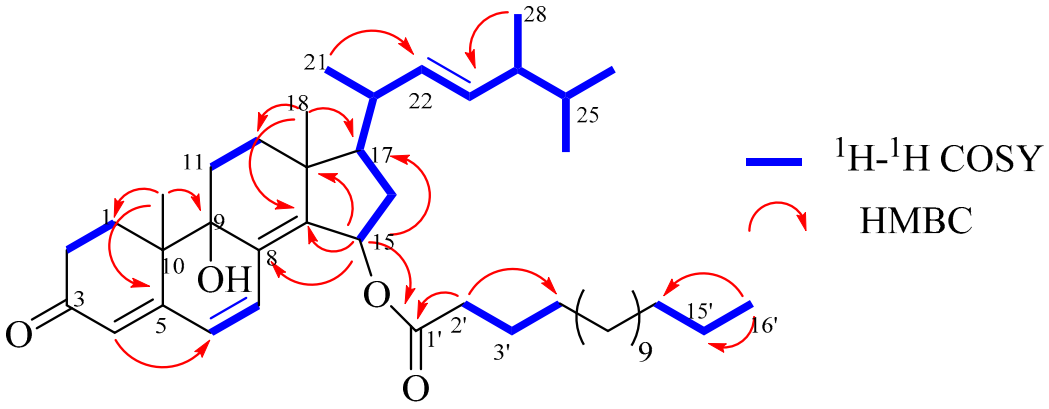

Figure 2. Key ^{1}H-^{1}H COSY and HMBC correlations of compound **1**.

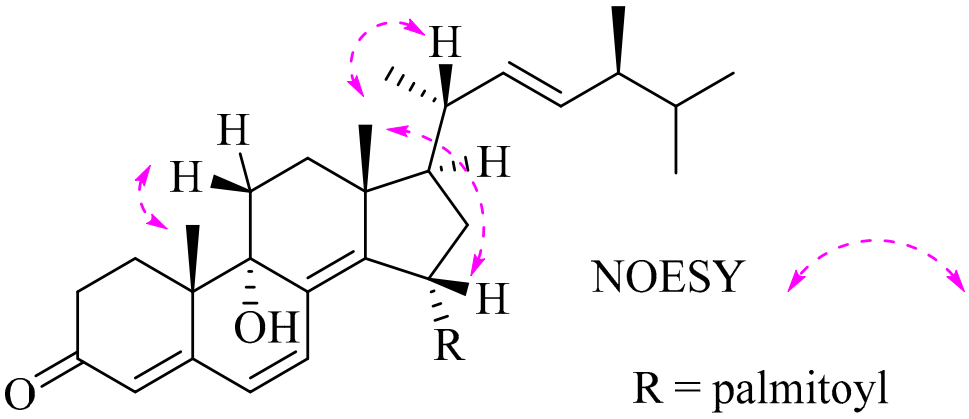

Figure 3. Key NOESY correlations of compound **1**.

Compounds **1**–**16** were assessed for their anti-inflammatory activity on the expression of pro-inflammatory cytokine factors *Tnfα* and *Ifnb1* in LPS- or DMXAA-induced Raw264.7 cells. Prior to exploring their anti-inflammatory properties, the potential toxicity of these compounds in Raw264.7 cells was evaluated to ensure that their effects were not confounded with cytotoxicity. The results demonstrated that most compounds had no significant impact on the viability of Raw264.7 cells, except for compounds **2**, **7**, and **16**, which exhibited some reduction in cell viability at high concentrations up to 40 μM (Figure 4).

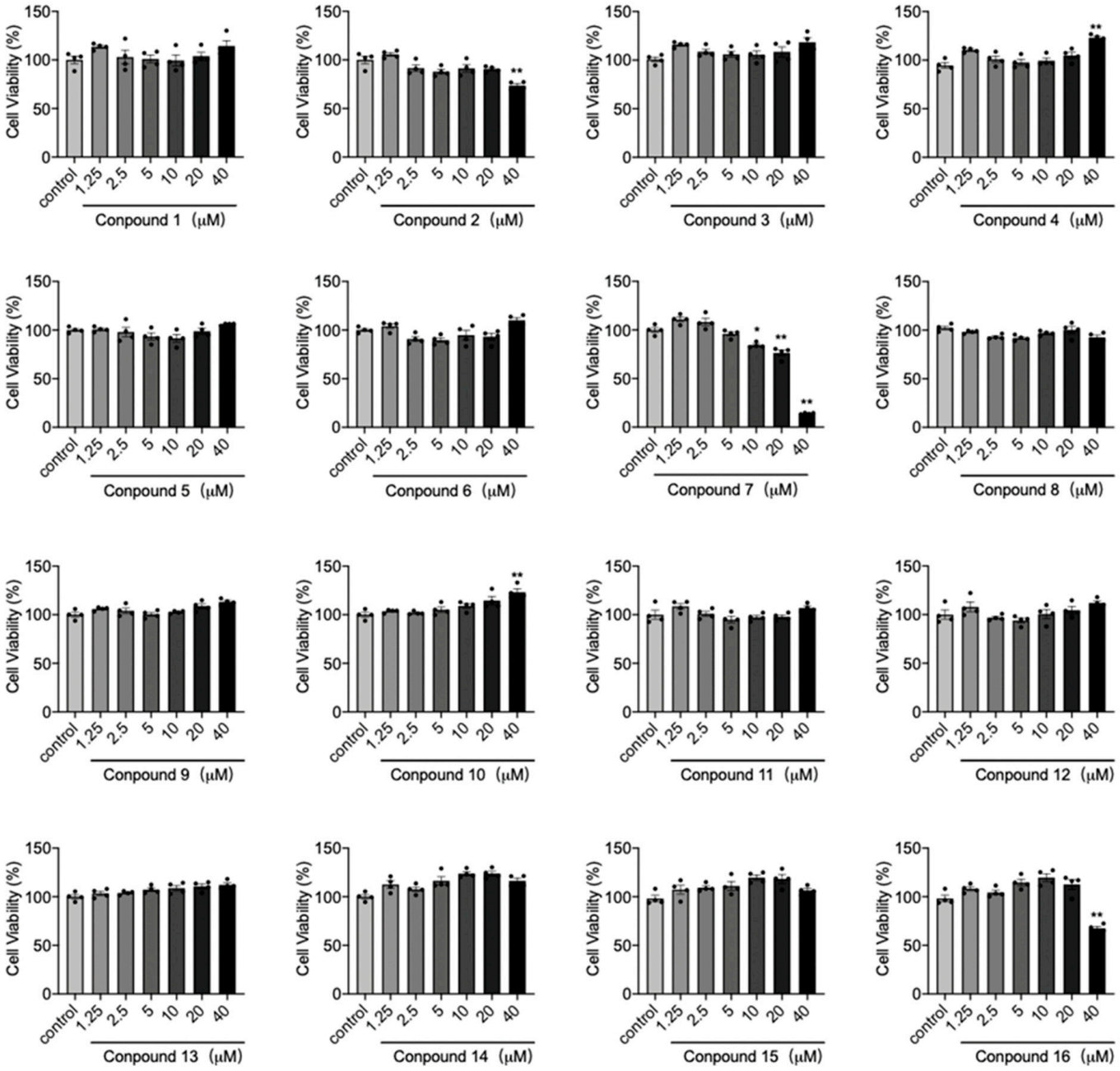

Figure 4. Raw264.7 cells were treated with compounds **1**–**16** at concentrations of 1.25, 2.5, 5, 10, 20, and 40 μM for 24 h. Cell viability was assessed using a cytotoxicity assay with CCK-8 reagent. * $p < 0.05$, ** $p < 0.01$ vs. control group, n = 4.

Cell apoptosis in macrophages is intricately associated with macrophage polarization, allowing macrophages to alter their phenotype and carry out diverse functions in response to changes in the microenvironment. The two main polarization states are classically activated macrophages (M1) and alternatively activated macrophages (M2). M1 macrophages exhibit characteristics such as pro-inflammatory mediator production, promotion of cell cytotoxicity, and antimicrobial abilities. Conversely, M2 macrophages possess anti-inflammatory properties, participate in tissue repair, regulate the immune response, and demonstrate anti-inflammatory capabilities. M1 macrophages induce cell death by releasing toxic molecules such as toxins, oxidants, and proteases, thereby augmenting their antimicrobial and antitumor effects. Nonetheless, excessive activation of M1 macrophages can result in tissue damage and inflammatory responses [44]. However, excessive activation

of M1 macrophages can lead to tissue damage and inflammatory responses. The experimental findings revealed that compound **7** exerted a more pronounced inhibitory effect on the survival of Raw264.7 cells at a concentration of 40 μM compared to other compounds. This suggests that compound **7** may promote the polarization of M1 macrophages while inhibiting the expression of growth-related proteins such as P38, Akt, and Wnt and promoting the expression of apoptosis-related genes such as Bcl-2, Bcl-xL, and Mcl-1. Consequently, this inhibits macrophage proliferation and promotes macrophage apoptosis. Moreover, the inhibitory effect of compound **7** on the viability of Raw264.7 cells at a concentration of 40 μM also suggests its potential to inhibit the proliferation and differentiation of tumor cells.

The expression of inflammatory factors in Raw264.7 cells, such as *Tnfα* and *Ifnb1*, which were stimulated by LPS, was suppressed by the administration of compounds **1**–**16** (Figure 5).

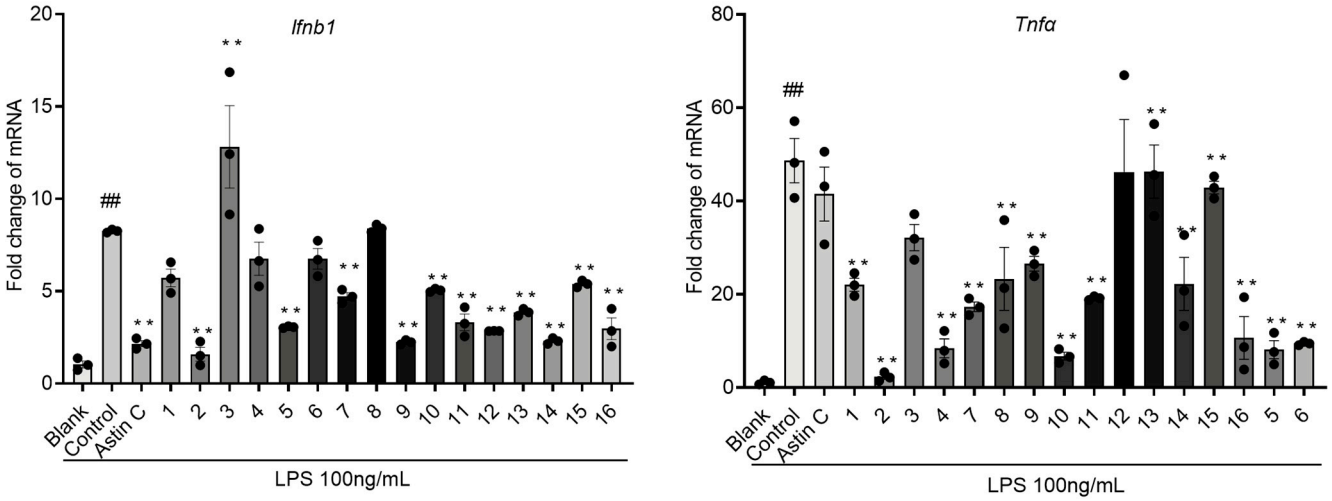

Figure 5. Raw264.7 cells were pretreated with compounds **1**–**16** at a concentration of 20 μM for 2 h. Subsequently, the cells were stimulated with LPS (100 ng/mL) for 6 h. Total RNA was then extracted from the cells and subjected to a quantitative real-time polymerase chain reaction (*q*RT-PCR) to analyze the expression of a panel of genes associated with the innate immune response. ** $p < 0.01$ vs. Control group; ## $p < 0.01$ vs. Blank group, n = 3.

The above results demonstrate that the compounds exhibit good inhibitory activity against type I interferon, and the cGAS-STING pathway in the innate immune response is an important mechanism for regulating type I interferon responses [45–47]. The expression levels of *Tnfα* and *Ifnb1* in the STING pathway have practical importance in immune regulation, inflammatory diseases, and therapeutic interventions, serving as key indicators of immune activation, effectiveness against pathogens, and the extent of inflammation [48,49]. Therefore, we further used the specific activator DMXAA of the cGAS-STING pathway to establish an activation model and evaluate the activity of these compounds. Using astin C (20 nM) as a positive control and a natural inhibitor of the STING pathway [50], the results indicate that all compounds significantly inhibit the expression levels of *Tnfα* and *Ifnb1* (Figure 6). In the stimulation of Raw264.7 cells with LPS, compounds **2**, **9**, and **14** showed significant inhibition of the inflammatory cytokine *Ifnb1* expression, while compounds **2**, **4**, and **5** exhibited strong inhibition of the inflammatory cytokine *Tnfα* expression. When Raw264.7 cells were stimulated with DMXAA, compounds **1**, **5**, and **7** effectively suppressed the inflammatory cytokine *Ifnb1* expression, whereas compounds **7**, **8**, and **11** demonstrated the best inhibition of the inflammatory cytokine *Tnfα* expression. Notably, newly isolated compounds **2** and **11** demonstrated potent anti-inflammatory activity. Hence, it is probable that compounds **1**–**16** exert their anti-inflammatory effects through the modulation of the cGAS-STING pathway.

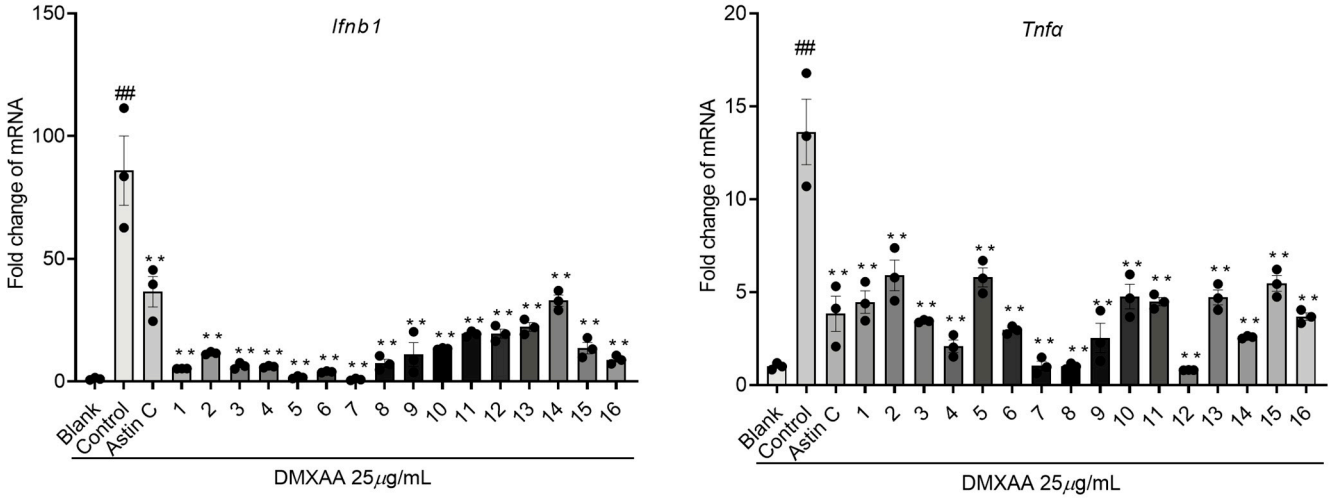

Figure 6. Raw264.7 cells were preincubated with compounds **1**–**16** (20 μM) and Astin C (20 nM) for a duration of 2 h, followed by stimulation with DMXAA (25 μg/mL) for 6 h. Total RNA was extracted from the cells and subjected to *q*RT-PCR analysis to evaluate the expression of a panel of genes associated with innate immune-responsive genes. ** $p < 0.01$ vs. Control group; ## $p < 0.01$ vs. Blank group, n = 3.

3. Materials and Methods

3.1. General Experimental Procedures

Optical rotations were determined with a Autopol VI polarimeter (Rudolph, Wood County, WI, USA). UV spectra and ECD spectra were taken in MeOH on a Jasco-715 spectropolarimeter. Infrared spectra were recorded on a Nicolet iN10 (micro) spectrometer (Thermo Fisher Scientific, Waltham, MA, USA). The NMR spectra were recorded on a Bruker DRX-600 (Bruker, Germany) spectrometer with chemical shifts reported relative to the residual $CDCl_3$ (δ_H 7.26 ppm, δ_C 77.0 ppm) and CD_3OD (δ_H 3.31 ppm; δ_C 49.0 ppm). The HRESIMS analyses were performed on a Q Exactive Plus Orbitrap (Thermo Fisher Scientific, Waltham, MA, USA) mass spectrometer. The UPLC-MS analysis of total ion chromatogram (TIC) was obtained using Agilent 1290 Infinity-6538 UHD (Agilent, Santa Clara, CA, USA) and Accurate-Mass QTOF/MS (Agilent, Santa Clara, CA, USA). Semipreparative HPLC was performed on a Waters 1525 (Waters, Milford, MA, USA) with a YMC Pack ODS-A column (250 × 10 mm, 5 μM; YMC, Kyoto, Japan). Sephadex LH-20 gel (GE Healthcare Bio-Sciences AB, Uppsala, Sweden) and silica gel (200–300 mesh, 300–400 mesh; Yantai Chemical Engineering Institure, Yantai, China) were used for column chromatography. Precoated silica gel plates (HSGF-254; Yantai Chemical Engineering Institure, Yantai, China) were used for thin-layer chromatography (TLC). Spots were detected on TLC under UV or by heating after spraying with an anisaldehyde sulfuric acid reagent.

3.2. Fungal Material

P. oxalicum HL-44 was isolated from the soft coral *S. gaweli* that was collected from the Xisha area of the South China Sea at a depth of 15 m in Aug 2018 and identified as *P. oxalicum* using 18sRNA sequence (GenBank accession number MG585101.1). A voucher strain of this fungus (internal strain No. HL-44) was deposited at Tongji University, Shanghai, China.

3.3. Screening Culture Medium and Cultivation

Five media, including Czapek Dox Agar (CZA) medium, Glucose Peptone Yeast (GPY) medium, Potato Dextrose Agar (PDA) medium, Rose Bengal Medium (RBM), and Rice medium, were used in the fermentation to compare the chemical diversity of fungal HL-44. UPLC-MS analysis of five extracts indicated that the PDA medium allowed the strain to produce metabolites with large molecular weights and more chemical diversity (m/z range

from 408 to 688, t_R from 10.5 to 14.5 min, Figure S2). The PDA medium was then selected for scale-up fermentation.

3.4. Extraction and Isolation

The culture medium containing mycelia was cut into small pieces and extracted five times ultrasonically with EtOAc to afford 43.5 g of residue after removal of the solvent under reduced pressure. The crude extract was separated into ten fractions (Fr.1–10) with silica gel CC (80 mm × 150 mm, 810 g, 200–300 mesh), eluting with a gradient CH_2Cl_2/MeOH (100:0 v/v 5 L, 80:1 v/v 3 L, 60:1 v/v 5 L, 40:1 v/v 3 L, 20:1 v/v 5 L, 5:1 v/v 5 L). Fr. 1 (3.3 g) was subjected to a Sephadex LH-20 CC (4 cm × 120 cm) using CH_2Cl_2/MeOH (v/v 2:1) as eluent to obtain eight subfractions (Fr.1a-h). Fr.1c (411.6 mg) was separated with silica gel CC (10 mm × 150 mm, 14 g, 300–400 mesh) using gradient petroleum (PE) in Me_2CO (39:1 v/v 40 mL, 24:1 v/v 50 mL, 19:1 v/v 40 mL, 1:1 v/v 20 mL), then split with HPLC to yield compound **1** (0.9 mg, MeOH/H_2O 98:2, 2 mL/min, t_R 64 min). Fr.1e (112.8 mg) was separated with silica gel CC (15 mm × 200 mm, 38 g, 300–400 mesh) using PE/Me_2CO (39:1 v/v 120 mL, 29:1 v/v 120 mL, 19:1 v/v 160 mL, 9:1 v/v 100 mL, 4:1 v/v 50 mL, 2:1 v/v 30 mL), then split with HPLC to yield compound **11** (1.6 mg, MeOH/H_2O 90:10, 2 mL/min, t_R 51 min) and compound **6** (12.8 mg, MeOH/H_2O 87:13, 2 mL/min, t_R 55 min). Fr.1f (788.1 mg) was separated with silica gel CC (20 mm × 150 mm, 55 g, 300–400 mesh) using PE/Me_2CO (39:1 v/v 100 mL, 19:1 v/v 100 mL, 14:1 v/v 120 mL, 9:1 v/v 100 mL, 1:1 v/v 50 mL), then split with HPLC to yield compound **14** (1.5 mg, MeOH/H_2O 88:12, 2 mL/min, t_R 74 min), compound **12** (0.6 mg, MeOH/H_2O 88:12, 2 mL/min, t_R 81 min) and compound **15** (8.4 mg, MeOH/H_2O 88:12, 2 mL/min, t_R 95 min). Fr. 2 (794.5 mg) was fractionated using Sephadex LH-20 CC (CH_2Cl_2/MeOH v/v 2:1, 4 cm × 120 cm) and then purified with silica gel CC (15 mm × 150 mm, 30 g, 300–400 mesh) using a gradient PE in Me_2CO (39:1 v/v 80 mL, 19:1 v/v 100 mL, 9:1 v/v 100 mL, 1:1 v/v 40 mL), and HPLC to afford compound **4** (2.8 mg, MeOH/H_2O 97:3, 2 mL/min, t_R 52 min) and compound **7** (4.4 mg, MeOH/H_2O 95:5, 2 mL/min, t_R 41 min). Fr. 4 (2.2 g) was fractionated using Sephadex LH-20 CC (CH_2Cl_2/MeOH v/v 2:1, 4 cm × 120 cm) and then purified with silica gel CC (20 mm × 150 mm, 55 g, 300–400 mesh) using a gradient PE in Me_2CO (29:1 v/v 90 mL, 19:1 v/v 100 mL, 14:1 v/v 90 mL, 9:1 v/v 100 mL, 4:1 v/v 50 mL) and HPLC to give compound **5** (4.4 mg, MeOH/H_2O 80:20, 2 mL/min, t_R 65 min), compound **3** (0.5 mg, CH_3CN/H_2O 70:30, 2 mL/min, t_R 185 min), and compound **16** (1.9 mg, MeOH/H_2O 80:20, 2 mL/min, t_R 73 min). Fr. 5 (755.9 mg) was fractionated using Sephadex LH-20 CC (CH_2Cl_2/MeOH v/v 2:1, 4 cm × 120 cm) and then purified with silica gel CC (15 mm × 150 mm, 30 g, 300–400 mesh) using a gradient PE in Me_2CO (29:1 v/v 90 mL, 14:1 v/v 90 mL, 9:1 v/v 120 mL, 4:1 v/v 50 mL) and HPLC to give compound **10** (1.8 mg, MeOH/H_2O 88:12, 2 mL/min, t_R 69 min). Fr. 7 (740.6 mg) was fractionated using Sephadex LH-20 CC (CH_2Cl_2/MeOH v/v 2:1, 4 cm × 120 cm) and then purified with silica gel CC (15 mm × 150 mm, 30 g, 300–400 mesh) using PE/Me_2CO (8:1 v/v 90 mL and 4:1 v/v 50 mL) to give compound **13** (2.0 mg). Fr. 9 (2.4 g) was fractionated using Sephadex LH-20 CC (CH_2Cl_2/MeOH v/v 2:1, 4 cm × 120 cm) and then purified with silica gel CC (10 mm × 150 mm, 14 g, 300–400 mesh) using PE/ Me_2CO (8:1 v/v 90 mL, 6:1 v/v 70 mL, 4:1 v/v 30 mL) and HPLC to give compound **2** (1.3 mg, MeOH/H_2O 87:13, 2 mL/min, t_R 27 min). Fr. 10 (1.7 g) was fractionated using Sephadex LH-20 CC (CH_2Cl_2/MeOH v/v 2:1, 4 cm × 120 cm) and then purified with silica gel CC (15 mm × 150 mm, 30 g, 300–400 mesh) using PE/Me_2CO (19:1 v/v 80 mL, 9:1 v/v 120 mL, 7:1 v/v 80 mL, 5:1 v/v 120 mL, 2:1 v/v 90 mL) and HPLC to give compound **9** (1.4 mg, MeOH/H_2O 90:10, 2 mL/min, t_R 35 min) and compound **8** (0.9 mg, MeOH/H_2O 90:10, 2 mL/min, t_R 47 min).

Characterization data of compound **1**: (22*E*,24*S*)-9α,15α-dihydroxyergosta-4,6,8(14),22-tetraen-3-one 15-palmitate (**1**): yellowish oil, $[\alpha]_D^{25}$ +43.40 (*c* 0.10, CH_3OH); UV (CH_3OH) λ_{max} (log ε) 330 (2.49), 265 (2.02) nm; ECD (CH_3OH, *c* 1.5 × 10^{-4}) λ_{max} (Δ ε) 241 (+1.80), 320 (-1.43), 361 (+2.76) nm; IR (micro) ν_{max} 3443, 2929, 2854, 1733, 1664, 1595, 1460, 1260,

1094, 1033, 970, 801 cm^{-1}; ^{1}H and ^{13}C NMR data see Table 1; HRESIMS m/z 663.53448 $[M + H]^+$ (calcd for $C_{44}H_{71}O_4$, 663.53469).

3.5. Cell Viability Detection

The viability of Raw264.7 cells was evaluated using the CCK-8 assay. Initially, the cells were seeded at a density of 3×10^4 cells/well in 96-well plates and allowed to incubate overnight. The cells were treated with the tested compounds at concentrations ranging from 1.25 to 40 μM for 24 h. After removing the culture medium, a CCK-8 solution diluted in Dulbecco's modified Eagle medium was added to each well. Following a 1-h incubation, the absorbance was measured at 450 nm using a multifunctional microplate spectrophotometer. Cell viability was then calculated as a percentage relative to the blank group [51].

3.6. Quantitative Real-Time PCR (qPCR)

Raw264.7 cells were pretreated with tested compounds at a concentration of 20 μM, along with astin C [50] at a concentration of 20 nM, for 2 h. Subsequently, the cells were stimulated with LPS at a concentration of 100 ng/mL and DMXAA at a concentration of 25 μg/mL for 6 h [52]. Total RNA was extracted from Raw264.7 cells using a triazole reagent supplied by Thermo Fisher Scientific. cDNA synthesis was performed using SuperScript III reverse transcriptase obtained from Invitrogen. Real-time PCR analysis was conducted using a PrimeScript RT reagent kit from Takara. The relative expression levels of the target genes were quantitatively normalized to the expression level of Gapdh using the ΔΔct method. Primer sequences are *Ifnb1*, forward 5′-GCACTGGGTGGAATGAGACT-3′ and reverse 5′-AGTGGAGAGCAGTTGAGGACA-3′; *Tnfα*, forward 5′-GTCCCCAAAGGGATGAGAAGTT-3′ and reverse 5′-GTTTGCTACGACGTGGGCTACA-3′ [52].

3.7. Statistical Analysis

The statistical analyses were conducted using GraphPad Prism 8.0. A one-way analysis of variance (ANOVA) was applied to the data, followed by Tukey's test for comparisons against the blank and control groups. A significance level of $p < 0.05$ was considered statistically significant.

4. Conclusions

With chemical analysis of the PDA medium extract of the fungus *P. oxalicum* HL-44 associated with the soft coral *S. gaweli*, a new ergostane-type sterol ester (**1**) was isolated together with fifteen derivatives (**2**–**16**). Their structures were determined using spectroscopic analyses and comparisons with reported data. This is the first report of compounds **2** and **11** from the family of Eurotiaceae. The isolation of ergosteroid derivatives with varying degrees of oxidation revealed a remarkable range of chemical diversity, expanding the ergosteroid family associated with this fungus. In an in vitro biotest, these compounds demonstrated potent anti-inflammatory activities at a concentration of 20 μM, effectively suppressing the expression of inflammatory factors such as *Tnfα* and *Ifnb1* in Raw264.7 cells induced with LPS or DMXAA. Among DMXAA-induced Raw264.7 cells, compounds **7** and **8** exhibited the highest level of inhibition in terms of *Tnfα* and *Ifnb1* expression. Conversely, in LPS-induced Raw264.7 cells, compounds **2** and **4** displayed the most pronounced inhibitory effects on *Tnfα* and *Ifnb1* expression. This study provides valuable insight into the chemical diversity of ergosteroid derivatives and their potential as anti-inflammatory agents.

Supplementary Materials: The following supporting information can be downloaded at https://www.mdpi.com/article/10.3390/molecules28237784/s1. Figure S1. HL-44 cultured on PDA medium (A), CZA medium (B), GPY medium (C), RBM, (D) Rice medium, and (E); Figure S2. Total Ion Chromatography (TIC) of 5 candidate media extracts: PDA medium (A), CZA medium (B), GPY medium (C), RBM (D), and Rice medium (E); Figures S3–S13. 1H-NMR, 13C-NMR, DEPT, 1H-1H COSY, HSQC, HMBC, NOESY, UV, IR, HRESIMS, and CD spectra of compound 1; Figure S14. OR data of compound 1 in CH3OH; Figure S15. The 1H-NMR spectrum of previously reported compounds **2**–**16**.

Author Contributions: C.P. performed the experiments. Y.-H.C. and H.-H.B. contributed to the bioassay. J.-P.Z. was responsible for the fungal fermentation. W.Z., H.H. and L.S. conceived and designed the experiments. All authors have read and agreed to the published version of the manuscript.

Funding: This research was funded by the National Natural Science Foundation of China (Nos. 81820108030, 82173735, and 82273937) and STCSM (21430711400).

Institutional Review Board Statement: Not applicable.

Informed Consent Statement: Not applicable.

Data Availability Statement: All data are available in the main text or the Supplementary Materials.

Conflicts of Interest: The authors declare no conflict of interest.

References

1. Cheung, R.C.F.; Ng, T.B.; Wong, J.H.; Chen, Y.; Chan, W.Y. Marine natural products with anti-inflammatory activity. *Appl. Microbiol. Biotechnol.* **2016**, *100*, 1645–1666. [CrossRef]
2. Zhabinskii, V.N.; Drasar, P.; Khripach, V.A. Structure and Biological Activity of Ergostane-Type Steroids from Fungi. *Molecules* **2022**, *27*, 2103. [CrossRef] [PubMed]
3. Kubatova, A.; Hujslova, M.; Frisvad, J.C.; Chudickova, M.; Kolarik, M. Taxonomic revision of the biotechnologically important species *Penicillium oxalicum* with the description of two new species from acidic and saline soils. *Mycol. Prog.* **2019**, *18*, 215–228. [CrossRef]
4. Zhang, P.; Li, X.-M.; Liu, H.; Li, X.; Wang, B.-G. Two new alkaloids from *Penicillium oxalicum* EN-201, an endophytic fungus derived from the marine mangrove plant *Rhizophora stylosa*. *Phytochem. Lett.* **2015**, *13*, 160–164. [CrossRef]
5. Zhang, R.; Ma, Y.; Xu, M.-M.; Wei, X.; Yang, C.-B.; Zeng, F.; Duan, J.-A.; Che, C.-T.; Zhou, J.; Zhao, M. Oxalactam A, a Novel Macrolactam with Potent Anti-Rhizoctonia solani Activity from the Endophytic Fungus Penicillium oxalicum. *Molecules* **2022**, *27*, 8811. [CrossRef] [PubMed]
6. Ren, Y.; Chao, L.-H.; Sun, J.; Chen, X.-N.; Yao, H.-N.; Zhu, Z.-X.; Dong, D.; Liu, T.; Tu, P.-F.; Li, J. Two new polyketides from the fungus *Penicillium oxalicum* MHZ153. *Nat. Prod. Res.* **2019**, *33*, 347–353. [CrossRef] [PubMed]
7. Weng, W.; Li, R.; Zhang, Y.; Pan, X.; Jiang, S.; Sun, C.; Zhang, C.; Lu, X. Polyketides isolated from an endophyte *Penicillium oxalicum* 2021CDF-3 inhibit pancreatic tumor growth. *Front. Microbiol.* **2022**, *13*, 1033823. [CrossRef] [PubMed]
8. Li, X.; Li, X.-M.; Zhang, P.; Wang, B.-G. A new phenolic enamide and a new meroterpenoid from marine alga-derived endophytic fungus *Penicillium oxalicum* EN-290. *J. Asian Nat. Prod. Res.* **2015**, *17*, 1204–1212. [CrossRef]
9. Zhang, Y.-H.; Li, L.; Li, Y.-Q.; Luo, J.-H.; Li, W.; Li, L.-F.; Zheng, C.-J.; Cao, F. Oxalierpenes A and B, unusual indole-diterpenoid derivatives with antiviral activity from a marine-derived strain of the fungus *Penicillium oxalicum*. *J. Nat. Prod.* **2022**, *85*, 1880–1885. [CrossRef]
10. Wang, Y.; Chen, W.; Xu, Z.; Bai, Q.; Zhou, X.; Zheng, C.; Bai, M.; Chen, G. Biological secondary metabolites from the *Lumnitzera littorea*-derived fungus *Penicillium oxalicum* HLLG-13. *Mar. Drugs* **2023**, *21*, 22. [CrossRef]
11. He, Z.-H.; Xie, C.-L.; Hao, Y.-J.; Xu, L.; Wang, C.-F.; Hu, M.-Y.; Li, S.-J.; Zhong, T.-H.; Yang, X.-W. Solitumergosterol A, a unique 6/6/6/6/5 steroid from the deep-sea-derived *Penicillium solitum* MCCC 3A00215. *Org. Biomol. Chem.* **2021**, *19*, 9369–9372. [CrossRef] [PubMed]
12. Tian, H.; Li, X.P.; Zhao, J.; Gao, H.W.; Xu, Q.M.; Wang, J.W. Biotransformation of artemisinic acid to bioactive derivatives by endophytic Penicillium oxalicum B4 from *Artemisia annua* L. *Phytochemistry* **2021**, *185*, 112682. [CrossRef] [PubMed]
13. de Queiroz, T.M.; Ellena, J.; Porto, A.L.M. Biotransformation of Ethinylestradiol by Whole Cells of Brazilian Marine-Derived Fungus *Penicillium oxalicum* CBMAI 1996. *Mar. Biotechnol.* **2020**, *22*, 673–682. [CrossRef] [PubMed]
14. Wang, H.L.; Li, R.; Li, J.; He, J.; Cao, Z.Y.; Kurtán, T.; Mándi, A.; Zheng, G.L.; Zhang, W. Alternarin A, a drimane meroterpenoid, suppresses neuronal excitability from the coral-associated fungi *Alternaria* sp. ZH-15. *Org. Lett.* **2020**, *22*, 2995–2998. [CrossRef]
15. Wang, H.L.; Li, R.; Zhao, M.; Wang, Z.Y.; Tang, H.; Cao, Z.Y.; Zheng, G.L.; Zhang, W. A drimane meroterpenoid borate as a synchronous Ca plus oscillation inhibitor from the coral-associated fungus *Alternaria* sp. ZH-15. *J. Nat. Prod.* **2023**, *86*, 429–433. [CrossRef]

16. Li, J.; Sun, Y.L.; Tang, H.; Su, L.; Zheng, G.L.; Zhang, W. Immunosuppressive 9,10-secosteroids from the gorgonian *Verrucella umbraculum* collected in the South China Sea. *J. Nat. Prod.* **2021**, *84*, 1671–1675. [CrossRef]
17. Shi, Q.; Huang, Y.; Su, H.; Gao, Y.; Peng, X.; Zhou, L.; Li, X.; Qiu, M. C(28) steroids from the fruiting bodies of *Ganoderma resinaceum* with potential anti-inflammatory activity. *Phytochemistry* **2019**, *168*, 112109. [CrossRef]
18. Weng, Y.F.; Lu, J.; Xiang, L.; Matsuura, A.; Zhang, Y.; Huang, Q.M.; Qi, J.H. Ganodermasides C and D, two new anti-aging ergosterols from spores of the medicinal mushroom *Ganoderma lucidum*. *Biosci. Biotechnol. Biochem.* **2011**, *75*, 800–803. [CrossRef]
19. Kwon, H.C.; Zee, S.D.; Cho, S.Y.; Choi, S.U.; Lee, K.R. Cytotoxic ergosterols from *Paecilomyces* sp. J300. *Arch. Pharmacal Res.* **2002**, *25*, 851–855. [CrossRef]
20. Liu, X.-H.; Miao, F.-P.; Liang, X.-R.; Ji, N.-Y. Ergosteroid derivatives from an algicolous strain of *Aspergillus ustus*. *Nat. Prod. Res.* **2014**, *28*, 1182–1186. [CrossRef]
21. Duecker, F.L.; Heinze, R.C.; Mueller, M.; Zhang, S.D.; Heretsch, P. Synthesis of the alleged structures of fortisterol and herbarulide and structural revision of herbarulide. *Org. Lett.* **2020**, *22*, 1585–1588. [CrossRef] [PubMed]
22. Amagata, T.; Tanaka, M.; Yamada, T.; Doi, M.; Minoura, K.; Ohishi, H.; Yamori, T.; Numata, A. Variation in cytostatic constituents of a sponge-derived *Gymnascella dankaliensis* by manipulating the carbon source. *J. Nat. Prod.* **2007**, *70*, 1731–1740. [CrossRef] [PubMed]
23. Fangkrathok, N.; Sripanidkulchai, B.; Umehara, K.; Noguchi, H. Bioactive ergostanoids and a new polyhydroxyoctane from *Lentinus polychrous* mycelia and their inhibitory effects on E2-enhanced cell proliferation of T47D cells. *Nat. Prod. Res.* **2013**, *27*, 1611–1619. [CrossRef] [PubMed]
24. Hoque, N.; Afroz, F.; Khatun, F.; Rony, S.R.; Hasan, C.M.; Rana, M.S.; Sohrab, M.H. Physicochemical, pharmacokinetic and cytotoxicity of the compounds Isolated from an endophyte *Fusarium oxysporum*: In vitro and in silico approaches. *Toxins* **2022**, *14*, 159. [CrossRef] [PubMed]
25. Wang, F.; Fang, Y.; Zhang, M.; Lin, A.; Zhu, A.; Gu, Q.; Zhu, W. Six new ergosterols from the marine-derived fungus *Rhizopus* sp. *Steroids* **2008**, *73*, 19–26. [CrossRef] [PubMed]
26. Tan, Z.; Zhao, J.-L.; Liu, J.-M.; Zhang, M.; Chen, R.-D.; Xie, K.-B.; Chen, D.-W.; Dai, J.-G. Lanostane triterpenoids and ergostane-type steroids from the cultured mycelia of *Ganoderma capense*. *J. Asian Nat. Prod. Res.* **2018**, *20*, 844–851. [CrossRef] [PubMed]
27. Gao, H.; Hong, K.; Chen, G.-D.; Wang, C.-X.; Tang, J.-S.; Yu, Y.; Jiang, M.-M.; Li, M.-M.; Wang, N.-L.; Yao, X.-S. New oxidized sterols from *Aspergillus awamori* and the endo-boat conformation adopted by the cyclohexene oxide system. *Magn. Reson. Chem.* **2010**, *48*, 38–43. [CrossRef]
28. Zhang, W.; Draeger, S.; Schulz, B.; Krohn, K. Ring B aromatic steroids from an endophytic fungus, *Colletotrichum* sp. *Nat. Prod. Commun.* **2009**, *4*, 1449–1454. [CrossRef]
29. Kim, K.H.; Choi, S.U.; Park, K.M.; Seok, S.J.; Lee, K.R. Cytotoxic constituents of *Amanita subjunquillea*. *Arch. Pharmacal Res.* **2008**, *31*, 579–586. [CrossRef]
30. Du, Z.-Z.; Shen, Y.-M. A rare new cleistanthane diterpene from the pericarp of *Trewia nudiflora*. *Helv. Chim. Acta* **2006**, *89*, 2841–2845. [CrossRef]
31. Yajima, A.; Kagohara, Y.; Shikai, K.; Katsuta, R.; Nukada, T. Synthesis of two osteoclast-forming suppressors, demethylincisterol A(3) and chaxine A. *Tetrahedron* **2012**, *68*, 1729–1735. [CrossRef]
32. Wang, Y.; Dai, O.; Peng, C.; Su, H.G.; Miao, L.L.; Liu, L.S.; Xiong, L. Polyoxygenated ergosteroids from the macrofungus *Omphalia lapidescens* and the structure-cytotoxicity relationship in a human gastric cancer cell line. *Phytochem. Lett.* **2018**, *25*, 99–104. [CrossRef]
33. Wright, J.L.C.; McInnes, A.G.; Shimizu, S.; Smith, D.G.; Walter, J.A.; Idler, D.; Khalil, W. Identification of C-24 alkyl epimers of marine sterols by C-13 nuclear magnetic-resonance spectroscopy. *Can. J. Chem.* **1978**, *56*, 1898–1903. [CrossRef]
34. Gao, H.; Hong, K.; Zhang, X.; Liu, H.-W.; Wang, N.-L.; Zhuang, L.; Yao, X.-S. New steryl esters of fatty acids from the mangrove fungus *Aspergillus awamori*. *Helv. Chim. Acta* **2007**, *90*, 1165–1178. [CrossRef]
35. Mahato, S.B.; Banerjee, S.; Podder, S. Steroid transformations by microorganisms-III. *Phytochemistry* **1989**, *28*, 7–40. [CrossRef]
36. Schlosser, D.; Schmauder, H.P. 15-alpha-hydroxylation of 13-ethyl-gon-4-ene-3,17-dione using a hyphal fungus immobilized in calcium alginate gel beads. *J. Basic Microbiol.* **1991**, *31*, 385–390. [CrossRef]
37. Irrgang, S.; Schlosser, D.; Fritsche, W. Involvement of cytochrome P-450 in the 15 alpha-hydroxylation of 13-ethyl-gon-4-ene-3,17-dione by *Penicillium raistrickii*. *J. Steroid Biochem. Mol. Biol.* **1997**, *60*, 339–346. [CrossRef] [PubMed]
38. Mao, S.H.; Wang, X.R.; Zhang, Z.H.; Wang, S.; Li, K.; Lu, F.P.; Qin, H.M. 15 alpha-hydroxylation of D-ethylgonendione by *Penicillium raistrickii* in deep eutectic solvents DESs containing system. *Biochem. Eng. J.* **2020**, *164*, 7781–7789. [CrossRef]
39. Krohn, K.; Biele, C.; Aust, H.J.; Draeger, S.; Schulz, B. Herbarulide, a ketodivinyllactone steroid with an unprecedented homo-6-oxaergostane skeleton from the endophytic fungus *Pleospora herbarum*. *J. Nat. Prod.* **1999**, *62*, 629–630. [CrossRef]
40. Yu, J.-H.; Yu, S.-J.; Liu, K.-L.; Wang, C.; Liu, C.; Sun, J.-y.; Zhang, H. Cytotoxic ergostane-type steroids from *Ganoderma lingzhi*. *Steroids* **2021**, *165*, 8767–8773. [CrossRef]
41. Liu, D.; Liu, J. Peroxy natural products. *Nat. Prod. Bioprospect.* **2013**, *3*, 161–206. [CrossRef]
42. Liu, D.; Li, X.-M.; Li, C.-S.; Wang, B.-G. Nigerasterols A and B, antiproliferative sterols from the mangrove-derived endophytic fungus *Aspergillus niger* MA-132. *Helv. Chim. Acta* **2013**, *96*, 1055–1061. [CrossRef]
43. Dericcardis, F.; Spinella, A.; Izzo, I.; Giordano, A.; Sodano, G. Synthesis of (17*R*)-17-methylincisterol, a highly degraded marine steroid. *Tetrahedron Lett.* **1995**, *36*, 4303–4306. [CrossRef]

44. Mills, C.D.; Lenz, L.L.; Harris, R.A. A breakthrough: Macrophage-directed cancer immunotherapy. *Cancer Res.* **2016**, *76*, 513–516. [CrossRef] [PubMed]
45. Wu, J.J.; Dobbs, N.; Yang, K.; Yan, N. Interferon-independent activities of mammalian STING mediate antiviral response and tumor immune evasion. *Immunity* **2020**, *53*, 115–126. [CrossRef] [PubMed]
46. Li, S.R.; Mirlekar, B.; Johnson, B.M.; Brickey, W.J.; Wrobel, J.A.; Yang, N.; Song, D.K.; Entwistle, S.; Tan, X.M.; Deng, M.; et al. STING-induced regulatory B cells compromise NK function in cancer immunity. *Nature* **2022**, *610*, 373–380. [CrossRef]
47. Haag, S.M.; Gulen, M.F.; Reymond, L.; Gibelin, A.; Abrami, L.; Decout, A.; Heymann, M.; van der Goot, F.G.; Turcatti, G.; Behrendt, R.; et al. Targeting STING with covalent small-molecule inhibitors. *Nature* **2018**, *559*, 269–273. [CrossRef]
48. Garland, K.M.; Sheehy, T.L.; Wilson, J.T. Chemical and biomolecular strategies for STING pathway activation in cancer immunotherapy. *Chem. Rev.* **2022**, *122*, 5977–6039. [CrossRef]
49. Wu, J.X.; Chen, Z.J. Innate immune sensing and signaling of cytosolic nucleic acids. *Annu. Rev. Immunol.* **2014**, *32*, 461–488. [CrossRef]
50. Li, S.L.; Hong, Z.; Wang, Z.; Li, F.; Mei, J.H.; Huang, L.L.; Lou, X.W.; Zhao, S.M.; Song, L.H.; Chen, W.; et al. The cyclopeptide Astin C specifically inhibits the innate immune CDN sensor STING. *Cell Rep.* **2018**, *25*, 3405–3421. [CrossRef]
51. Service, R.F. SYNTHETIC BIOLOGY Fluorine-adding bacteria may transform natural product medicines. *Science* **2013**, *341*, 1052–1053. [PubMed]
52. Chen, Y.; Bian, H.; Lv, J.; Song, W.; Xing, C.; Hui, C.; Zhang, D.; Zhang, C.; Zhao, L.; Li, Y.; et al. Gelsevirine is a novel STING-specific inhibitor and mitigates STING-related inflammation in sepsis. *Front. Immunol.* **2023**, *14*, 1190707. [CrossRef] [PubMed]